Extracellular electron transfer mechanism in Shewanella loihica PV- 4 biofilms formed at indium tin oxide and graphite electrodes

Journal Item

Int. J. Electrochem. Sci., 8 **(2013)** 1778 - 1793

International Journal of
ELECTROCHEMICAL
SCIENCE
www.electrochemsci.org

Extracellular Electron Transfer Mechanism in *Shewanella loihica* PV- 4 Biofilms Formed at Indium Tin Oxide and Graphite Electrodes.

Anand Jain[1,2], *Jack O Connolly*[3], *Robert Woolley*[4], *Satheesh Krishnamurthy*[5], *Enrico Marsili*[1,*,]

[1] School of Biotechnology, National Centre for Sensor Research, Dublin City University, Dublin 9, Ireland
[2] Biological Oceanography Division, National Institute of Oceanography, Goa, India
[3] School of Physics, National Centre for Plasma Science and Technology, Dublin City University, Dublin 9, Ireland
[4] Optical Sensor Laboratory, National Centre for Sensor Research, Dublin City University, Dublin 9, Ireland
[5] Department of Design Development Environment and Materials, The Open University, MK7 6AA, UK
[*]E-mail: enrico.marsili@dcu.ie

Received: 25 December 2012 / *Accepted:* 11 January 2013 / *Published:* 1 February 2013

Electroactive biofilms are capable of extracellular electron transfer to insoluble metal oxides and electrodes; such biofilms are relevant to biogeochemistry, bioremediation, and bioelectricity production. We investigated the extracellular electron transfer mechanisms in *Shewanella loihica* PV-4 viable biofilms grown at indium tin oxide (ITO) and graphite electrodes in potentiostat-controlled electrochemical cells poised at 0.2 V vs. Ag/AgCl. Chronoamperometry and confocal microscopy showed higher biofilm growth at graphite compared to the ITO electrode. Cyclic voltammetry, differential pulse voltammetry, along with fluorescence spectroscopy showed that direct electron transfer through outer membrane c type cytochromes (Omcs) prevailed at the biofilm/ITO interface, while biofilms formed at graphite electrode reduced the electrode also via secreted redox mediators, such as flavins and quinones. The biofilm age does not affect the prevalent transfer mechanism at ITO electrodes. On the other hand, secreted redox mediators accumulated at biofilm/graphite interface, thus increasing mediated electron transfer as the biofilm grows over five days. Our results showed that the electrode material determined the prevalent electron transfer mechanism and the dynamic of secreted redox mediators in *S. loihica* PV-4 biofilms. These observations have implications for the optimization of biofilm-based electrochemical systems, such as biosensors and microbial fuel cells.

Keywords: Extracellular Electron Transfer, *Shewanella loihica* PV- 4, Electroactive biofilms, ITO electrode, Graphite electrode.

1. INTRODUCTION

Dissimilatory metal reducing bacteria (DMRB) are capable of reducing insoluble metal oxides and hydroxides at circumneutral pH as a part of their energy generating strategy [1]. The most commonly studied DMRB include the members of *Shewanella* and *Geobacter* genus. *Shewanella* genus was important for carbon cycling and finds application in bioremediation and microbial fuel cells (MFCs) [2-5]. *Shewanella* can transfer electrons extracellularly to various electron acceptors, including Fe (III) and Mn (IV), nitrate, oxygen [6], and even protons for hydrogen production [7]. With respect to other electrochemically active biofilm (EAB)-forming bacteria, such as the strict anaerobe *Geobacter*, the facultative anaerobe *Shewanella* has a more adaptable metabolism and can grow on carbon-based and metal oxides electrodes [8-11]. Extracellular electron transfer (EET) in *Shewanella* genus occurs via Omcs [12], conductive pili [13], and excreted redox compounds, such as flavins and quinones [14]. The concurrence of direct electron transfer (DET) via Omcs and mediated electron transfer (MET) via excreted redox mediator was proven both in metal reduction and bioelectricity production [15-17]. Recent genetic and electrochemical analysis suggests that the EET mechanism in *Shewanella* genus might be specie-specific [2, 18]. Thus, characterization of EET mechanism in several species of the *Shewanella* genus is needed.

S. loihica PV-4 was isolated from an iron-rich microbial mat near a deep-sea hydrothermal vent located on the Loihi Seamount in Hawaii [20]. This strain has been characterized phenotypically and phylogenetically [2], and its metal reduction and biomineralization capabilities have also been reported [6]. When *S. loihica* PV-4 was grown under controlled laboratory conditions, they produced higher current than *S. oneidensis* MR-1 [17], thus they are relevant to fundamental studies, as well as to the design of efficient bioelectrochemical systems (BESs). Omcs seemed to be the key EET agent in *S. loihica* PV-4 [21]. However, these Omcs were differently utilized as compared to other *Shewanella* strains. *S. loihica* PV- 4 produced quinones and flavin derivatives [14, 17] under anaerobic growth conditions. While *S. oneidensis* MR-1 utilize flavins as redox mediators to shuttle electrons to electrode/metal oxides [9, 14, 16], the involvement of redox mediators in EET to electrode/metal oxides has not been demonstrated for *S. loihica* PV- 4.

Surface topography and chemistry of the electrode material determine the current output in *S. loihica* PV-4 biofilms [10, 19]. We propose that the electrode material select the EET mechanism in *S. loihica* PV-4 biofilms. To test this hypothesis, we grew *S. loihica* PV- 4 biofilms on ITO and commercial graphite electrode, in potentiostat-controlled ECs. Because of its small surface roughness and excellent optoelectronics properties, ITO is widely used for spectroelectrochemical characterization of purified redox proteins [23-24] and whole microbial cells [21, 25-26]. On the other hand, graphite has high surface roughness and is the most cost-effective material for BES. We then applied electrochemical, microscopy, and spectroscopy methods to unveil the complex EET mechanisms in *S. loihica* PV-4 at different biofilm ages.

2. EXPERIMENTAL PROCEDURE

2.1. Bacteria and growth medium

S. loihica PV- 4 strain (DSM 17748) was purchased from German Collection of Microorganisms and Cell Cultures (DSMZ), Germany. The culture was grown aerobically for 24 h at 30 ºC in Luria-Bertani medium (LB). The culture was then centrifuged at 13,400 rpm for 20 min, and the LB medium was replaced with defined medium containing per litre: $NaHCO_3$, 2.5 g, $CaCl_2 \cdot 2H_2O$, 0.08 g, NH_4Cl, 1.0 g, $MgCl_2 \cdot 6H_2O$, 0.2 g, NaCl 10 g, HEPES, 7.2 g. Vitamins mixture and trace metal solution were added to the defined medium, and 15 mM (mmol/L) lactate (final concentration) was added to the medium as electron donor [6]. The cells were grown aerobically in defined medium at 30 ºC for 2 days, under shaking condition at 150 rpm. Following centrifugation for 20 min at 13,400 rpm, the pellet was washed three times with defined medium containing 15 mM lactate, to remove soluble redox mediators (SRM) from the inoculum.

2.2. Electrode preparation

Commercial ITO sheet (Sigma-Aldrich, Ireland) (60 ohms/sq. resistivity) was cut into 2 cm ×1 cm size electrodes and the graphite sheet (Tokai Co, Japan) was cut into 2 cm ×1 cm × 0.2 cm size electrodes. The ITO sheet is conductive only from one side, thus the conductive surface area of ITO electrode was 2 cm^2. The graphite electrodes were polished by sandpaper (400 particles/ inch), cleaned in 1M HCl overnight, and stored in deionised (DI) water. The conductive surface area of graphite electrode used in this study was 5.2 cm^2. The current density values on ITO and graphite electrode was calculated by dividing the current values (obtained during chronoamperometry) with the conductive surface area of the respective electrodes.

2.3. Electrochemical setup and analyses

Single chamber jacketed electrochemical cells (ECs) of 10 ml working volume with three electrodes configuration were used [8, 9]. The Ag/AgCl reference electrode was connected to the EC via a saturated KCl salt bridge ending in a 3 mm Vycor glass membrane (Bioanalytical Systems, UK). All electrochemical potentials are described versus Ag/AgCl reference electrode (Fisher Scientific, Ireland), unless otherwise indicated. A 0.1 mm Pt wire (Sigma–Aldrich, Ireland) was used as the counter electrode. The working electrodes (graphite or ITO) were attached to the potentiostat via Pt wire, nylon screw and nut (Small Part, USA). The assembled EC was mounted on the magnetic stirrer, maintained at a constant speed of 150 rpm. The headspace of the EC was continuously flushed with humidified, sterile N_2, which had been passed over a heated copper column to remove trace oxygen. The EC was maintained at 30 ºC throughout the experiment and the working electrode was continuously poised at 0.2 V. The EC was connected to a VSP 5-channel potentiostat (Bio-Logic, France). *S. loihica* PV-4 biofilms formed at ITO and graphite electrodes were characterized by chronoamperometry (CA), cyclic voltammetry (CV), and differential pulse voltammetry (DPV). The

parameters for the techniques were chosen as it follows: CV: scan rate, 1 mV/s; E_i = -0.8 V; E_f = 0.2 V; DPV: E_i = -0.8 V and E_f = 0.2 V; pulse height, 50 mV; pulse width, 300 ms; step height, 2 mV; step time, 500 ms; scan rate, 4 mV/s; accumulation time, 5s. CV and DPV were performed approximately after every 24 h.

2.4. Biofilm growth on ITO and graphite electrodes

The washed *S. loihica* PV- 4 cell suspension was adjusted to optical density ($OD_{520\ nm}$) = 2.0 ± 0.2, then purged for 30 min with N_2, and finally 5 ml of this suspension were added to the EC filled with 5 ml of defined medium, to a final lactate concentration of 15 mM. After 24h, the spent growth medium was replaced with the fresh defined medium. Following the first medium change, the medium was replaced approximately after every 24 h. At least three independent experiments were performed on both ITO and graphite electrodes.

2.5. Fluorescence spectroscopy

Fluorescence spectroscopy of the spent medium collected from the EC with ITO and graphite working electrodes was performed using a LS-50B luminescence spectrometer (Perkin Elmer, USA). The spent medium was first centrifuged at 13,400 rpm for 20 minutes, and then filter-sterilized via 0.22 μm filter (Millipore, USA). The fluorescence excitation spectra (200 – 400 nm) at 430 nm emission wavelength and emission spectra (350 – 600 nm) at 360 nm excitation wavelength were also recorded. The excitation and emission slit widths were 2.5 nm with photomultiplier tube voltage of 600V. Data collection and post processing were performed by FL-WinLab Software (Perkin-Elmer, USA).

2.6. Confocal microscopy

S. loihica PV- 4 biofilms grown at ITO and graphite electrode was collected approximately after 120 h of growth in EC cells. The samples were removed from the EC in an anaerobic chamber (Coy Laboratory, USA), followed by staining for 30 min in 1 mg ml^{-1} acridine orange. After rinsing with defined medium to eliminate excess dye, the samples were fixed to a glass slide. The confocal images were captured with a laser scanning microscope (Zeiss LSM 510, USA), using argon laser 488 nm as excitation source. The objective was a plan apochromatic 63 x oil immersion, with numerical aperture 1.40. The fluorescence was recorded with a low pass filter at 505 nm. A series of images were taken along the biofilm thickness (Z axis) at 0.5 μm interval.

2.7. Atomic force microscopy

Tapping mode atomic force microscopy (AFM) of the bare ITO and graphite electrode was performed using Dimension 3100 (Bruker, USA). The average surface roughness (rms) was calculated via windows scanning (where x =force) microscope (WSxM) software [27].

3. RESULTS AND DISCUSSION

3.1. Electrochemistry of S. loihica PV- 4 biofilms formed at ITO electrode

An oxidation current density of 0.5 ± 0.3μA cm^{-2} was observed at ITO electrode immediately after inoculation of *S. loihica* PV-4 cell suspension (Figure 1).

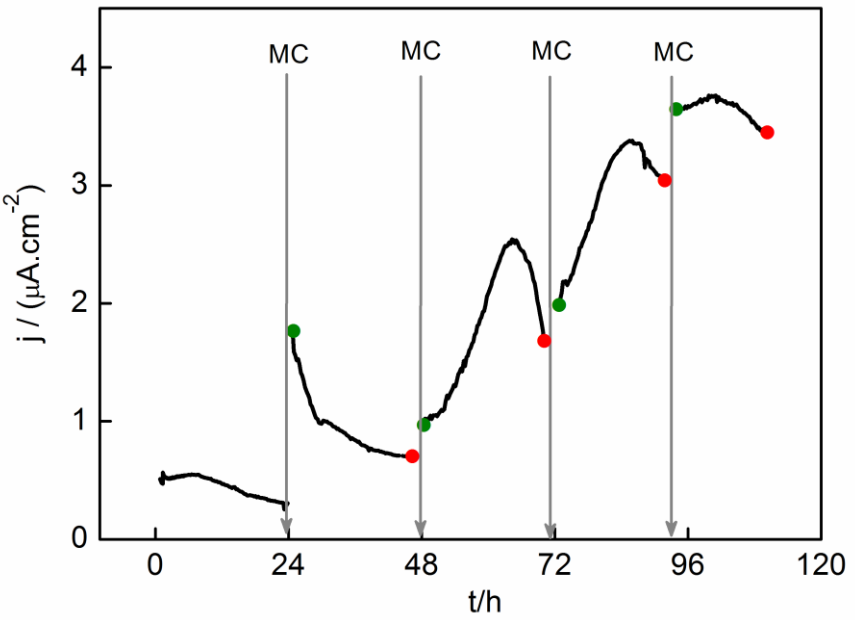

Figure 1. CA of *S. loihica* PV-4 at ITO electrode poised at oxidative potential (0.2 V vs. Ag/AgCl). Medium change (MC) was performed after every 24 h (approximately). CV and DPV were performed immediately before (●) and immediately after medium change (●).

The current increased after the second medium change at 48 h, and kept increasing until it reached a plateau of 3.7 ± 1.5μA cm^{-2} at 100 h. Previous studies reported a current of 1μA cm^{-2} [21]. As the conductivity of commercial ITO thin films varies with their thickness and crystallinity [28], we cannot easily compare our current output with previous literature. However, we choose a low resistivity (60 ohms/sq.) commercially available ITO for elucidating EET mechanism in *S. loihica* PV-4 biofilms. Thus, it is unlikely that the low current observed (with respect to that reported for graphite electrodes) is due to the ITO conductivity. Current density drops were observed at 64 h, 85 h and 100 h (Fig. 1). Current drop during bioelectrochemical experiments are caused by electron donor limitation, accumulation of metabolites, and/or pH change in the medium [29-32]. In our case, electron donor limitation was unlikely, since less than 1% lactate was converted into anodic current (Table 1). Additionally, the pH remained approximately 7.0 throughout the experiment and suspended cell concentration – expressed as protein concentration - was always very low (data not shown). Therefore, the current drops observed were likely due to the instability of *S. loihica* PV-4 biofilms formed at the ITO electrode.

Table 1. Charge generated and lactate converted to acetate, during *S. loihica* PV-4 growth on ITO electrode poised at 0.2 V vs. Ag/AgCl.

Duration	Charge (C)*	Lactate consumption** (mM)
0-24h	9.7	0.02
25-46h	18	0.04
47-72h	39	0.1
73-92h	53	0.13
93-110h	56	0.145

* The charge was calculated by integrating the current generated over a period of time

** Lactate conversion to acetate

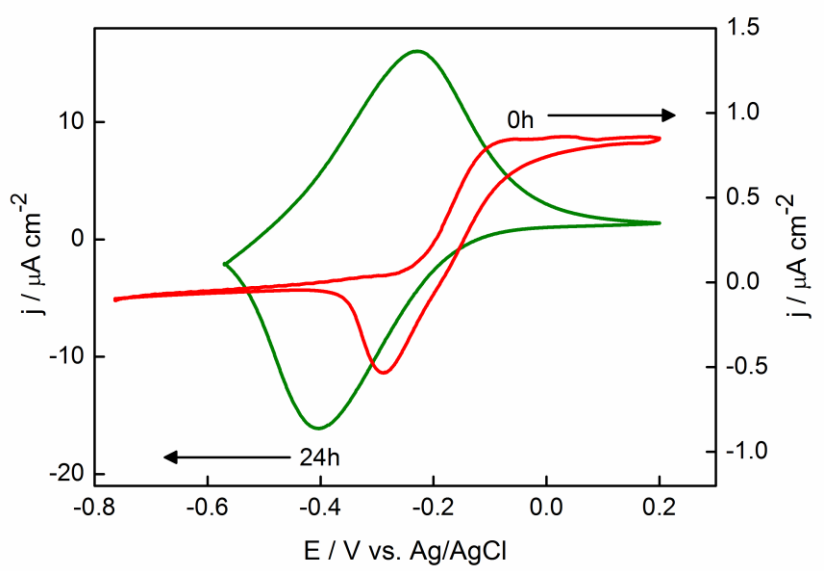

Figure 2. CV of *S. loihica* PV- 4 cell suspension (a) immediately after inoculation (red trace) and (b) 24h after inoculation (green trace). Scan rate: 1 mVs^{-1}.

CV of *S. loihica* PV- 4 cell suspension after inoculation showed a strong cathodic peak at -0.28V over-imposed on a well defined sigmoidal (turnover) curve (Figure 2). The turnover curve was due to the high concentration of suspended cells, thus of Omcs, as soluble redox mediators (SRM) were removed during the preparation of the inoculum. The large (irreversible) cathodic peak was due to the partial oxidation of Omcs during the cell suspension preparation procedure. The sigmoidal wave, onset at -0.27 V and centered at -0.15 V, indicated catalytic electron transfer by Omcs at the ITO/electrode interface [21]. After 24 h from inoculation, the sigmoidal wave disappeared and cyclic voltammetry detected reversible peaks with E_m value -0.3 V, most likely due to the production of redox mediator(s) in the cell suspension under anaerobic conditions. Anodic current increased as the microbially produced flavins accumulated and adsorbed at the electrode [9]. It appeared that electrons were transferred preferentially by DET via OmcA/MtrC complex of the attached *S. loihica* PV- 4 cells. It has been suggested that at positive electrode potential, DET mechanism is favored in *S. loihica* PV-4 cells attached on to ITO electrode [33]. Subsequent medium change restored the sigmoidal catalytic

wave in the CV and the maximum current increased after each medium change, indicating a build-up of the biofilm and an increased turnover rate (Figure 3A and 3B).

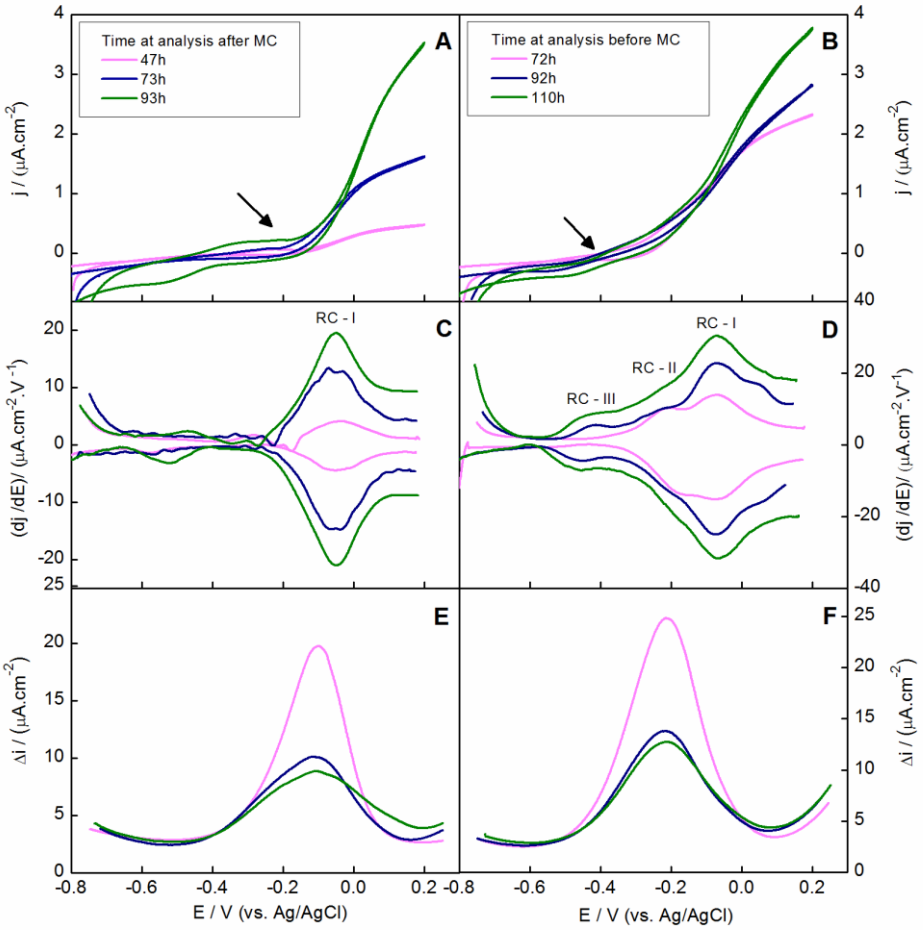

Figure 3. (A, B) CV, (C, D) derivative of CV and (E, F) DPV of *S. loihica* PV-4 biofilms at ITO electrode obtained immediately (A, C, E) after medium change and (B, D, F) just before medium change. The black arrow in (A) and (B) represent the onset potential of the CVs. (D) The derivative of CV before medium change show three redox centers RC-I=−0.06 V, RC-II=−0.2 V, and RC-III=−0.45 V while (C) derivative of CVs obtained after medium change shows only RC- I = -0.06 V. (E) DPV after medium change and (F) before medium change show a main redox process at -0.1 V and -0.2 V, respectively. "Δi" represents the difference between current values before and at the end of pulse in DPV.

The first order derivative of the CVs obtained immediately after medium change showed nearly symmetrical peaks centered at mid point potential of -0.06 V (Figure 3C). However, the derivative of the CVs obtained before medium change detected three redox centers RC (I) = -0.06V, RC (II) = -0.2V and RC (III) = -0.4 V (Fig. 3D). The potential of RC (II) and RC (III) were close to the midpoint potential of the quinone derivatives (-0.27 V) [17] and riboflavin (-0.42 V) [9], which are common redox mediators secreted by *Shewanella sp*. The accumulation of redox mediator(s) was also evident from the shift of the sigmoidal curve onset potential immediately before the medium change (Figure 3B). However, the role of these mediators in EET to the ITO electrode is not clear. It has been proved

that the cell-bound mediator menaquinone is not involved in the EET at *S. oneidensis* MR-1 biofilm/ITO electrode interface [34]. From the relative height of the two sigmoidal curves, most of the electrons were transferred at RC (I) = -0.06 V, which was close to the midpoint potential of the Omcs reported earlier from the whole cell voltammetry of *S. loihica* PV- 4 (-0.054 V vs. Ag/AgCl) [18] as well as of *S. oneidensis* MR-1 (-0.07 V vs. Ag/AgCl) [29]. The E_m value obtained for RC (I) was shifted to a more positive potential from those reported earlier for the multi-heme *c* type cytochromes purified from strain *S. oneidensis* MR-1. A possible explanation is that in viable microbial cells electrons are continuously supplied to the Omcs through oxidation of lactate, differently from what happen with purified proteins. This displaces the equilibrium to generate reduced form of Omcs, thereby shifts the E_m towards the positive potential [21]. Moreover, biofilm formation, concentration of biofilm-bound mediator(s) and pH- gradient at biofilm/electrode interface may also affect the formal potential of the major redox centre [35]. DPV detected only one peak at -0.2 V, whose potential shift at -0.1V after medium change (Figure 3E and 3F). We carried out a control experiment to determine whether these peaks corresponded to a specific flavin, especially riboflavin (RF) (Figure 4A).

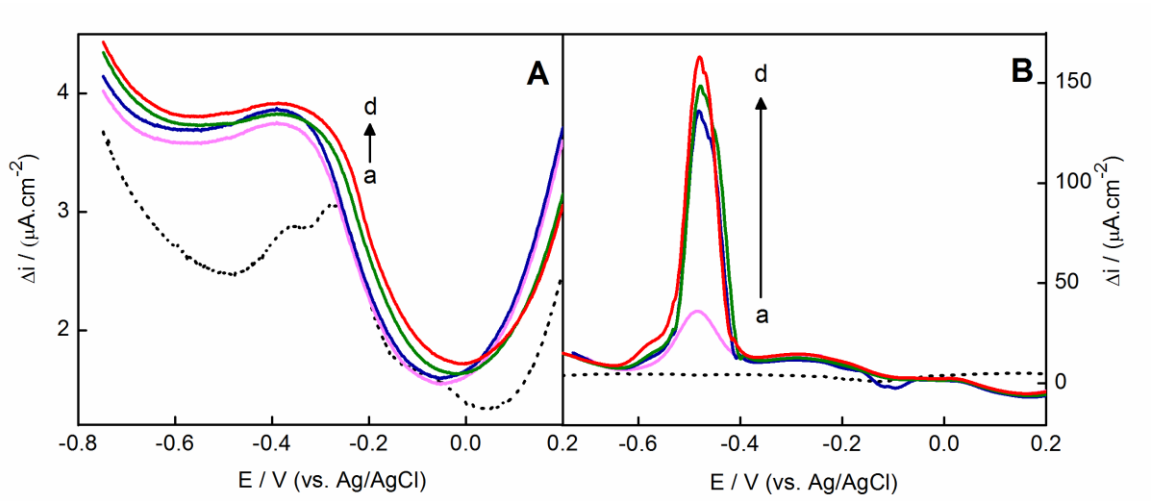

Figure 4. DPV of sterile (A) ITO and (B) graphite electrode after incubation in 1 µM riboflavin (RF) solution. The dotted line in A and B represents the blank (without riboflavin) and (a) 0h, (b) 8h, (c) 16h, and (d) 24h represents time of DPV analysis. The RF peak at -0.36 V and -0.44V was observed on ITO and graphite electrode, respectively. From the relative peak height, it appeared that RF concentration at graphite electrode is ~100 times higher than that at ITO electrode.

As RF on ITO produced a broader peak at -0.36 V (Figure 4), we concluded that the DPV peak observed for biofilms grown on ITO did not correspond to flavins, but to another electroactive species. Interestingly, the height of these peaks (at -0.2V and -0.1V) was not correlated to the current density, (Figure 5). In fact, the increasing current density was not due to the electroactive species with the peaks at -0.2 and -0.1V. However, flavins were observed in the supernatant associated to the ITO biofilms (Figure 10).

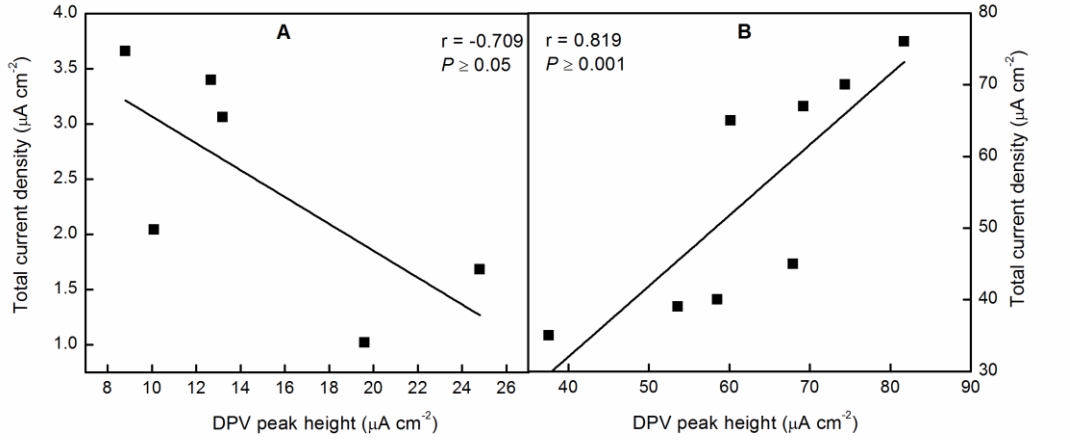

Figure 5. DPV peak height versus current density for *S. loihica* PV-4 biofilms formed at (A) ITO and (B) graphite electrode. Note that the DPV peak height and current density shows negative and positive correlation on ITO and graphite electrode, respectively.

In conclusion, although *S. loihica* PV- 4 biofilms formed at ITO electrode produced redox mediators, EET mechanism was prevalently direct and occurred via Omcs with E_m value -0.06V vs. Ag/AgCl.

3.2. Electrochemistry of S. loihica PV- 4 biofilms formed at graphite electrode

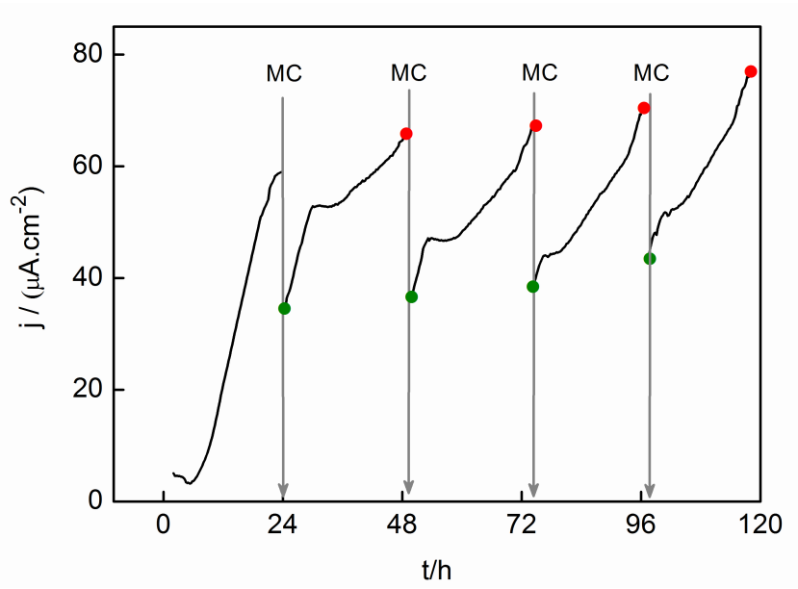

Figure 6. CA of *S. loihica* PV-4 biofilm at graphite electrode. Medium change (MC) was performed after every 24 h (approximately). CV and DPV were performed before (●) and after medium change (●).

CA of *S. loihica* PV- 4 biofilms on graphite electrode is shown in Figure 6. The current density of 5 ± 1.2μA cm^{-2} observed immediately after inoculation was 10 times higher than that measured on

ITO electrode. The high rms of the graphite electrodes (1.8 ± 0.4 µm) with respect to ITO electrodes (10 ± 2 nm) (Figure 7A and 7B) resulted in rapid cell attachment, as seen by the disappearance of the lag phase in current density (Figure 6) [32].

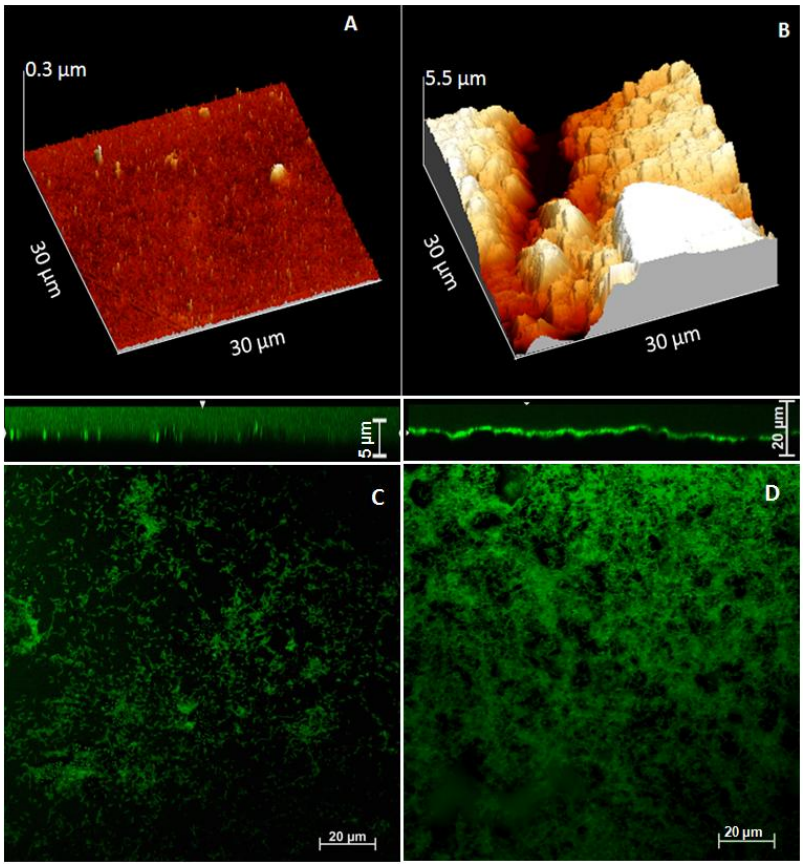

Figure 7. AFM pictures shown in 3D projection for (A) bare ITO and (B) graphite electrode. Confocal microscopy pictures of 120 h old *S. loihica* PV-4 biofilms formed at (C) ITO and (D) graphite electrode.

The maximum current density on graphite (75 ± 14 µA cm^{-2}) was approximately 20 times more than observed at ITO. *S. loihica* PV-4 formed sub-monolayered biofilms on ITO electrode (Figure 7C), compared to the 2-3 µm thick biofilm on graphite electrode (Figure 7D). The 50 ± 10 % drops in the original current after each medium change confirmed that the SRM transferred electrons from *S. loihica* PV-4 biofilms to electrode. Newton et al [17] observed approximately 50% drop in the current density after placing the anode containing *S. loihica* PV- 4 biofilm in a MFC containing fresh medium. In a separate experiment where spent defined medium was removed, centrifuged, filtered through 0.22 µm filters to remove planktonic cells, and then returned to EC containing *S. loihica* PV- 4 biofilms, the current was immediately restored to 94 ± 3 % of its original level (Figure 8). Thus, SRM mediated electron transfer from the biofilm cells to the graphite electrode accounted for the 50 % of the total current. This could be explained by the fact that not all the cells in a multi-layered biofilm (2-3 µm) are in direct contact with the electrode and the cells in the top biofilm layers use secreted SRM such as

flavins to transfer electrons to the electrode. The average cell size of *S. loihica* PV- 4 grown under anaerobic condition is approximately 1.6 × 0.4 μm [6]. Assuming that all the cells in biofilm were arranged parallel to the electrode surface, the biofilm would consist of 7-8 cell layers. Our results were consisting with those reported for a multi-layered biofilm of *Pseudomonas aeruginosa* KRP1 on graphite electrode [36], where the microorganisms use SRM to transfer electrons from top biofilm layers to the graphite electrode surface.

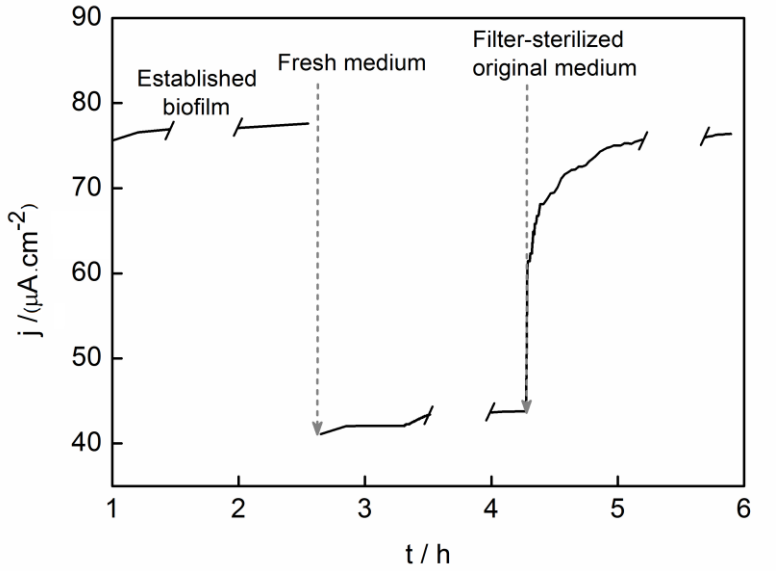

Figure 8. CA of 96 h old *S. loihica* PV- 4 biofilm at graphite electrode after medium change with fresh medium, and after adding the filter-sterilized original medium back in the EC. The gap in the CA represents the CV and DPV analysis.

Interestingly, the slope of current vs. time increased after subsequent medium change (Figure 6), indicating that the number of biofilm cells capable of transferring electrons to the graphite electrode, either through DET or MET, increased with time (Table 2).

Table 2. Calculated slope of current in a semi-logarithmic plot after initial current increase until subsequent medium change and its corresponding current duplication time for *S. loihica* PV-4 biofilms formed at graphite electrode.

Time after inoculation (h)	S	g (h)
24-48	0.00489	62
49-74	0.00666	45
74-96	0.00989	31
97-118	0.01	30

S = slope of current vs. time

g = current duplication time (h).

The turnover CV of *S. loihica* PV- 4 biofilm on graphite collected after medium change showed two overlapping catalytic waves, which onset at -0.6 V and -0.2 V and were centred at -0.45 V, and -0.05 V, respectively. CV indicated that two simultaneous catalytic electron transfer processes occurred at the biofilm/graphite interface (Figure 9A and 9B). Similar catalytic curves were reported for *S. oneidensis* MR-1 strain on graphite electrode [36], with the low potential and the high potential curve attributed to MET and to DET, respectively. The first derivative of the *S. loihica* PV-4 CVs showed the presence of three putative redox centers: RC (I) = -0.04 V, RC (II) = -0.35V, and RC (III) = -0.45V (Figure 9C and 9D), similar to the redox centers observed on ITO (Fig. 3B). However, the peak height at RC (III) increased with time, indicating a prevalence of MET over DET, as biofilm grew (Figure 9C and 9D). The decrease in RC (III) peak following medium change suggests that the redox mediators produced by *S. loihica* PV- 4 cells were removed in the medium change. This was supported by the DPV data (Figure 9F), which also indicated the accumulation of flavins and their removal through each medium change (Figure 9E). A significant linear correlation ($P \geq 0.01$) between DPV peak height at RC (III) and current density showed that the electrons were transferred mainly via MET in *S. loihica* PV-4 biofilm formed at graphite electrode (Figure 5).

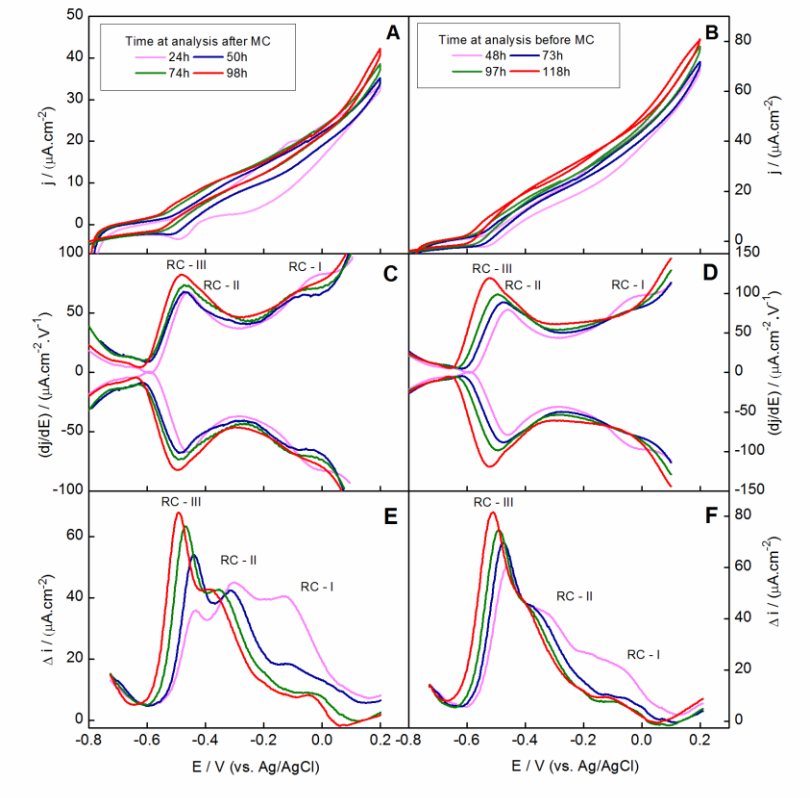

Figure 9. (A, B) CV, (C, D) derivative of CV and (E, F) DPV of *S. loihica* PV-4 biofilms at graphite electrode obtained immediately (A, C, E) after medium change and (B, D, F) just before medium change. (C, D) The derivative of CV (C) after medium change and (D) before medium change show three redox centers RC-I=−0.04 V, RC-II=−0.35 V, and RC-III=−0.45 V. (E) DPV after medium change and (F) before medium change show a increase in the peak height at RC-III with the incubation period. "Δi" represents the difference between (I) current values before and at the end of pulse in DPV.

The accumulation of flavins at the graphite interface explained the increase in the slope of current vs. time after subsequent medium change i.e., BRM accumulation at electrode interface increased overall EET rate. It is generally consider that anode-attached cells employ DET mechanisms, as is the case with *Geobacter* [29-30], while organisms employing MET are able to thrive as planktonic cells in MFCs [37]. Kouzuma et al [38] suggested that when cells are physically distant from the solid electron acceptors, MET is limited by the diffusion of the mediator compounds, thus the formation of biofilms could lead to more efficient current generation through a combination of DET and MET. However, selection of EET mechanism depends also on other factors, such as surface properties of the electrode material. Graphite/carbon electrode has high adsorption affinity for the biomolecules such as flavins [9]. Adsorbed flavins at the graphite interface might decrease interaction between Omcs and the electrode surface, thus favouring MET, as reported earlier [33, 39]. To quantify flavins adsorption at ITO and graphite electrodes, we incubated sterile electrodes in 1μM riboflavin solution for 24 h and monitored its adsorption through DPV (Figure 4B). The riboflavin peaks on graphite increase with time, much faster than the corresponding peaks on ITO. This result explains in part the lower current production and the minor contribution of MET at ITO electrode.

In conclusion, *S. loihica* PV-4 biofilm used both SRM and BRM along with Omcs for transferring electrons to the graphite anode. Approximately 50 % of the current produced by *S. loihica* PV-4 on graphite electrodes biofilm came from MET via SRM irrespective of the biofilm age. The rest of the current depended on the biofilm age. In young biofilms, current was produced by both DET via Omcs and MET via BRM . However, as the biofilm grew accumulation of redox mediators (such as flavins) at the biofilm/graphite interface resulted in prevalent MET (Figure 9E).

3.3. Fluorescence spectroscopy of the cell-free supernatants

To confirm the presence of soluble redox mediators in the spent medium associated with ITO and graphite anodes, the cell-free supernatants were analyzed with the fluorescence spectroscopy. The emission spectra collected at different times (Figure 10B and 10D) showed two peak emission wavelengths at 440 and 520 nm, similar to those of quinone derivatives (430 nm) and flavins (520 nm), respectively [10]. The presence of quinone derivatives in the ITO- and graphite-associated supernatants was further confirmed by excitation spectra (Figure 10A and 10C), where the major peak at 350 nm corresponded to the quinone derivatives [17]. The fluorescence peak intensity of ITO-associated supernatant at 440 and 520 nm decreased with time, while the fluorescence peak of graphite-associated supernatant at 520 nm (flavins peak) did not change significantly with time. This might be due to the continuous production of flavins by the *S. loihica* PV-4 cells, which compensated the amount of flavins in the medium removed after each medium change.

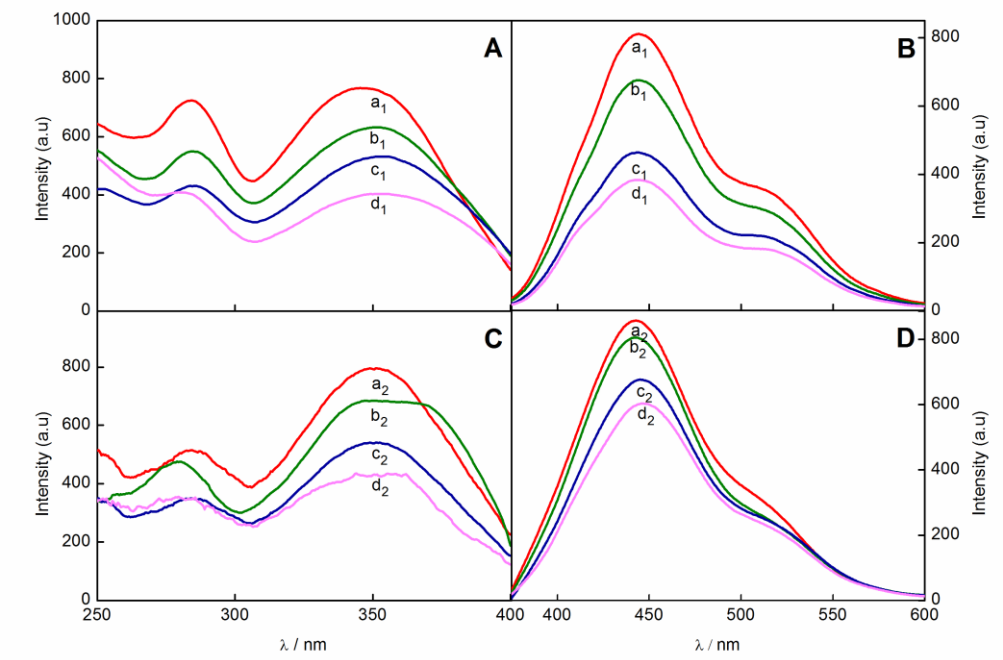

Figure 10. (A, C) Fluorescence excitation and (B, D) emission spectra of the cell free supernatant from *S. loihica* PV-4 biofilms associated with ITO {collected at (a_1) 24 h, (b_1) 48 h, (c_1) 72 h, and (d_1) 94 h after medium change} and graphite electrode {collected at (a_2) 24 h, (b_2) 49 h, (c_2) 74 h, and (d_2) 98 h after medium change}. The (B, D) emission spectra show the quinone peak at 441 nm and riboflavin peak at 520 nm in the both supernatants. The (A, C) excitation spectra confirm the presence of quinone derivatives at 350 nm.

4. CONCLUSIONS

Shewanella electroactive biofilms are capable of both direct and mediated EET. Our results show that the dominant EET mechanism depends on the electrode material on which biofilms are grown. *S. loihica* PV-4 biofilm show predominant DET at ITO electrodes and mixed DET/MET when grown on graphite electrodes. ITO has low affinity for flavins and low surface roughness that do not favor neither adsorption of microbially produced mediators nor microbial adhesion. Conversely, graphite higher affinity towards flavins and high surface roughness allow mediator adsorption and formation of a thicker biofilm, which in turn favors MET over DET at biofilm/graphite interface. We suggest that surface chemistry and topography of the electrode material play a pivotal role in deciding the prevalent EET mode at *Shewanella* biofilm/electrode interface.

ACKNOWLEDGEMENTS
Anand Jain is supported by the IRCSET EMPOWER post-doctoral fellowship. Enrico Marsili is supported by the EU-FP7 Marie Curie International Reintegration Grant.

References

1. D.R. Lovley, *Microbiol. Rev*., 55 (1991) 259-287.
2. J.K. Fredrickson, M.F. Romine, A.S. Beliaev, J.M. Auchtung, M.E. Driscoll, T.S. Gardner, K.H. Nealson, A.L. Osterman, G. Pinchuk, J.L. Reed, D.A. Rodionov, J.L. Rodrigues, D.A. Saffarini, M.H. Serres, A.M. Spormann, I.B. Zhulin, J.M. Tiedje, *Nat. Rev. Microbiol*., 6 (2008) 592-603.
3. M. Firer-Sherwood, G.S. Pulcu, S.J. Elliott, *J. Biol. Inorg. Chem*., 13 (2008) 849-854.
4. H.H. Hau, J.A. Gralnick, *Annu. Rev. Microbiol*., 61 (2007) 237-258.
5. J.C. Biffinger, L.A. Fitzgerald, R. Ray, B.J. Little, S.E. Lizewski, E.R. Petersen, B.R. Ringeisen, W.C. Sanders, P.E. Sheehan, J.J. Pietron, J.W. Baldwin, L.J. Nadeau, G.R. Johnson, M. Ribbens, S.E. Finkel, K.H. Nealson, *Bioresource. Technol.*, 102 (2011) 290-297.
6. Y. Roh, H. Gao, H. Vali, D.W. Kennedy, Z.K. Yang, W. Gao, A.C. Dohnalkova, R.D. Stapleton, J.W. Moon, T.J. Phelps, J.K. Fredrickson, J. Zhou, Appl. Environ. Microbiol, 472 (2006) 3236-3244.
7. G. Meshulam-Simon, S. Behrens, A.D. Choo, A.M. Spormann, *Appl. Environ. Microbiol*., 73 (2007) 1153-1165.
8. A. Jain, X. Zhang, G. Pastorella, N. Berry, J. O'Connolly, R. Woolley, S. Krishnamurthy, E. Marsili, *Bioelectrochem*., 87(2012) 28-32.
9. E. Marsili, D.B. Baron, I.D. Shikhare, D. Coursolle, J.A. Gralnick, D.R. Bond, *Proc. Natl. Acad. Sci. USA*, 105 (2008) 3968-3973.
10. Y. Zhao, K. Watanabe, R. Nakamura, S. Mori, H. Liu, K. Ishii, K. Hashimoto, *Chem. Eur. J*., 16 (2010) 4982-4985.
11. J. Connolly, A. Jain, G. Pastorella, S. Krishnamurthy, J. P. Mosnier, E. Marsili, *Virulence*, 2 (2011) 5.
12. B.H. Kim, H.J. Kim, M.S. Hyun, D.H. Park, *J. Microbiol. Biotechnol*., 9 (1999) 127-131.
13. Y.A. Gorby, S. Yanina, J. S. McLean, K. M. Rosso, D. Moyles, A. Dohnalkova, T. J. Beveridge, I. S. Chang, B. H. Kim, K. S. Kim, D. E. Culley, S. B. Reed, M. F. Romine, D. A. Saffarini, E. A. Hill, L. Shi, D. A. Elias, D.W. Kennedy, G. Pinchuk, K. Watanabe, S. Ishii, B. Logan, K. H. Nealson, and J. K. Fredrickson, *Proc. Natl. Acad. Sci. USA*, 103 (2006) 11358-11363.
14. H. Von Canstein, J. Ogawa, S. Shimizu, J.R. Lloyd, *Appl. Environ. Microbiol*., 74 (2008) 615-623.
15. J.K. Hyung, S.P. Hyung, S.H. Moon, S.C. In, K. Mia, H.K. Byung, *Enzyme Microb. Technol*., 30 (2002) 145-152.
16. D. Coursolle, D.B. Baron, D.R. Bond, J.A. Gralnick, *J. Bacteriol*., 192 (2010) 467-474.
17. G.J. Newton, S. Mori, R. Nakamura, K. Hashimoto, K. Watanabe, *Appl. Environ. Microbiol*., 75 (2009) 7674-7681.
18. O. Bretschger, A.C.M. Cheung, F. Mansfeld, K.H. Nealson, *Electroanal*., 22 (2010) 883- 894.
19. Y. Zhao, S. Nakanishi, K. Watanabe, K. Hashimoto, *J. Biosci. Bioeng.*, 112 (2011) 63-66.
20. H. Gao, A. Obraztova, N. Stewart, R. Popa, J.K. Fredrickson, J.M. Tiedje, K.H. Nealson, J. Zhou, *Int. J. Syst. Evol. Microbiol.*, 56 (2006) 1911-1916.
21. R. Nakamura, K. Ishii, K. Hashimoto, *Angew. Chem. Int. Ed*., 48 (2009) 1606 -1608.
22. Y. Astuti, E. Topoglidis, G. Gilardi, J.R. Durrant, *Bioelectrochem*., 63 (2004) 55-59.
23. Y. Astuti, E. Topoglidis, P.B. Briscoe, A. Fantuzzi, G. Gilardi, J.R. Durrant, *J. Am. Chem. Soc*., 126 (2004) 8001-8009.
24. J.P. Busalmen, A. Esteve-Nuñez, A. Berná, J.M. Feliu, *Bioelectrochem*., 78 (2010) 25-29.
25. A. Jain, G. Gazzola, A. Panzera, M. Zanoni, E. Marsili, *Electrochim. Acta*, 56 (2011) 10776-10785.
26. I. Horcas, R. Fernandez, J.M. Gomez-Rodriguez, J. Colchero, J. Gomez-Herrero, A. M. Baro, *Rev. Sci. Instrum*., 78 (2007) 013705-8.
27. D.H. Kim, M.R. Park, H.J. Lee, G.H. Lee, *Appl. Surf. Sci*., 253 (2006) 409-411.

28. E. Marsili, J.B. Rollefson, D.B. Baron, R.M. Hozalski, D.R. Bond, *Appl. Environ. Microbiol.*, 74 (2008) 7329-7337.
29. E. Marsili, J. Sun, D.R. Bond, *Electroanal.*, 22 (2010) 865-874.
30. K. Fricke, F. Harnisch, U. Schroder, *Energy Environ. Sci*., 1 (2008) 144-147.
31. C. Dumas, R. Basseguy, A. Bergel, *Electrochim. Acta*, 53 (2008) 5235-5241.
32. H. Liu, S. Matsuda, S. Kato, K. Hashimoto, S. Nakanishi, *Chem. Sus. Chem*., 3 (2010) 1253-1256.
33. A. Okamoto, R. Nakamura, K. Hashimoto, *Electrochim. Acta*, 56 (2011) 5526-5531.
34. A.A. Carmona-Martinez, F. Harnisch, L.A. Fitzgerald, J.C. Biffinger, B.R. Ringeisen, U. Schröder, *Bioelectrochem*., 81 (2011) 74-80.
35. K. Rabaey, N. Boon, M. Hofte, W. Verstraete, *Environ. Sci. Technol*., 39 (2005) 3401-3408.
36. U.Schroder, *Phys. Chem. Chem. Phys*., 9 (2007) 2619–2629.
37. A. Kouzuma, X.Y. Meng, N.Kimura, K. Hashimoto, K. Watanabe, *Appl. Environ. Microbiol.*, 76 (2010) 4151- 4157.
38. L. Peng, S.J. You, J.Y. Wang, *Biosens. Bioelectron.*, 25 (2010) 2530-2533.